

UNCLASSIFIED

~~CONFIDENTIAL~~

Copy 5
RM E57D01

3 1176 01351 8080

NACA RM E57D01

NACA

RESEARCH MEMORANDUM

SOME REYNOLDS NUMBER PHENOMENA

IN A TURBOJET COMPRESSOR

By Harold R. Kaufman

Lewis Flight Propulsion Laboratory
Cleveland, Ohio

CLASSIFICATION CHANGED

UNCLASSIFIED

To

LIBRARY COPY

By authority of *NACA TPA 8* *Effective*
Date *7-22-57*
NB 9-10-59

JUN 28 1957

LANGLEY AERONAUTICAL LABORATORY
LIBRARY, NACA
LANGLEY FIELD, VIRGINIA

CLASSIFIED DOCUMENT

This material contains information affecting the National Defense of the United States within the meaning of the espionage laws, Title 18, U.S.C., Sec. 793 and 794, the transmission or revelation of which in any manner to an unauthorized person is prohibited by law.

NATIONAL ADVISORY COMMITTEE FOR AERONAUTICS

WASHINGTON

June 26, 1957

~~CONFIDENTIAL~~ UNCLASSIFIED

NATIONAL ADVISORY COMMITTEE FOR AERONAUTICS

RESEARCH MEMORANDUM

SOME REYNOLDS NUMBER PHENOMENA IN A TURBOJET COMPRESSOR

By Harold R. Kaufman

SUMMARY

An investigation was conducted with a compressor of a current turbo-jet engine to determine the effects of Reynolds number variations on some boundary-layer phenomena. The compressor was instrumented to obtain first-stage and over-all compressor performance. Also, instrumentation was installed at the midspan position on the inlet guide vanes and first-stage stators to measure the boundary-layer profiles and suction-surface velocity distributions. The range of first-rotor Reynolds number investigated was from about 3×10^4 to 4×10^5 . For the compressor investigated, this range of Reynolds number corresponded to an altitude range from about 35,000 to 85,000 feet at a flight Mach number of 0.8.

At low Reynolds numbers, laminar separation regions were found on the inlet guide vanes. The use of boundary-layer trippers on the inlet guide vanes greatly reduced or eliminated these laminar separation regions and increased the over-all compressor efficiency and airflow 1 to 2 percent at low Reynolds numbers. At high Reynolds numbers, the use of inlet-guide-vane trippers resulted in about a 1-percent drop in compressor efficiency and no change in airflow.

The midspan flow on the first stator was essentially turbulent at all Reynolds numbers, probably because of the high turbulence level within the compressor. The use of boundary-layer trippers on all compressor blades therefore does not appear promising.

The losses of the complete compressor vary inversely as about the one-fifth power of Reynolds number, which is in agreement with turbulent boundary-layer theory. Thus, with the exception of the first one or two blade rows, the losses within a compressor apparently come from turbulent-boundary-layer phenomena. However, further knowledge of compressor losses, particularly in the hub and tip regions, is needed before this conclusion can be put on a rigorous basis.

INTRODUCTION

Although it is generally accepted that the boundary layer is responsible for Reynolds number effects on compressor performance, the actual

boundary-layer phenomena are not clear. From the Reynolds number range in which turbojet compressors operate, laminar separation and turbulent reattachment has been suspected as the cause of Reynolds number effects. On the other hand, the turbulence level is high within a compressor, which should reduce the extent of laminar flow and the possibility of laminar separation. An investigation was conducted to determine the effect of compressor Reynolds number variations on some boundary-layer phenomena, particularly laminar separation regions, and the role they play in Reynolds number effects.

The compressor used in the investigation was instrumented to obtain first-stage and over-all compressor performance. Also, instrumentation was installed at the midspan position on the inlet guide vanes and first-stage stators to measure the boundary-layer profiles and suction-surface velocity distributions. In an attempt to improve the flow through the inlet guide vanes, boundary-layer trippers were installed for part of the investigation.

An inherent limitation to the data should be pointed out. All boundary-layer and suction surface instrumentation was installed at about the midspan position. Hence, the flow phenomena observed do not represent a complete and conclusive picture of three-dimensional losses in a compressor.

To avoid off-design problems (which are beyond the scope of this report) the investigation was restricted to rated corrected engine speed and rated compressor pressure ratio. The range of Reynolds number (based on the chord at the tip of the first rotor) was from about 3×10^4 to 4×10^5 . For the compressor investigated, this range of Reynolds number corresponded to an altitude range from about 35,000 to 85,000 feet at a flight Mach number of 0.8.

Investigations of the effects of Reynolds number on airfoil boundary layers have, in the past, been restricted almost entirely to isolated airfoils. The presentation herein therefore contains comparisons to isolated airfoil experience. A short summary of Reynolds number effects on isolated airfoils is included to aid in these comparisons.

SYMBOLS

c	chord
H	boundary-layer form factor, $\hat{\delta}^*/\theta$
K	constant
n	Reynolds number exponent

V	velocity
V_s	suction-surface velocity (outside of boundary layer)
$V_{s,max}$	maximum suction-surface velocity
V_0	velocity outside of boundary layer
V_1	velocity upstream of blade row
V_2	velocity downstream of blade row
ΔV	mean velocity fluctuation
w	weight flow
x	distance from leading edge
y	distance from blade surface
δ	ratio of compressor-inlet total pressure to NACA standard sea-level pressure of 2116 lb/sq ft or 29.92 in. Hg abs
$\hat{\delta}$	boundary-layer thickness (to point where velocity is 99 percent of free-stream value)
$\hat{\delta}^*$	boundary-layer displacement thickness, $\hat{\delta}^* = \int_0^\infty \left(1 - \frac{V}{V_0}\right) dy$ (density assumed constant)
η	adiabatic compressor efficiency
θ	ratio of compressor-inlet total temperature to NACA standard sea-level temperature of 518.7° R
$\hat{\theta}$	boundary-layer momentum thickness, $\hat{\theta} = \int_0^\infty \frac{V}{V_0} \left(1 - \frac{V}{V_0}\right) dy$ (density assumed constant)
μ	absolute viscosity
ρ	density

APPARATUS AND PROCEDURE

Apparatus

Compressor. - A 13-stage axial-flow turbojet compressor was used for the investigation. The rated pressure ratio was about 6.9. The midspan chord lengths of the inlet guide vanes, first rotor, and first stator (after the first rotor) were 1.25, 2.0, and 1.4 inches.

Instrumentation. - Conventional pressure and temperature instrumentation was installed at the inlet and outlet of the compressor to determine over-all compressor performance. Pressure and temperature measurements were also made after the first rotor to permit calculation of first-stage performance.

Boundary-layer total-pressure surveys were made near the trailing edges of the inlet guide vanes and first stators at about the midspan position. Although this instrumentation is shown only for the inlet guide vanes in figures 1 and 2, the instrumentation was similar for the first stator. The static-pressure distribution on the suction surfaces of these two blade rows was also measured at the midspan position (fig. 2).

The plane of the boundary-layer survey was slightly upstream of the trailing edges (at about the 81-percent-chord position) to avoid the effects of radial flow. Experience has shown that radial flow of the low-energy boundary layer often occurs downstream of a blade row. On a blade surface, however, the boundary-layer shear forces generally prevent any large radial components of velocity.

Boundary-layer trippers. - The tripper configuration used in this investigation was a spanwise wire located on the suction surface near the leading edge and was developed in a separate investigation in a low-velocity duct with only a portion of the inlet-guide-vane annular cascade. The tripper wires were optimized in diameter and chordwise position at three radii to give the smallest suction-surface displacement thickness at the minimum Reynolds number of the complete compressor investigation. The optimum configuration was without a wire on the one-third of the span closest to the hub, had a wire diameter-to-chord ratio of 0.015 on the middle third, and a ratio of 0.022 on the outer third. The optimum position of the wires was just behind the plane of the leading edges. These tripper wires can be seen in figures 1 and 2. The trippers (copper wire) were soldered to the steel inlet guide vanes.

Although the duct test was run at sea-level density with very low velocities to simulate the desired Reynolds number, excellent agreement of boundary-layer profiles was obtained with the over-all compressor tests (both with and without trippers), indicating that the combined effects of different free-stream Mach numbers and turbulence levels were small. The duct investigation was conducted for the sole purpose of

developing a practical tripper configuration. Hence, no data from the duct investigation are shown in the present report.

Procedure

The compressor performance was obtained with the compressor operating as an integral component of a current 8000-pound-thrust-class turbojet engine. The engine was installed in the 20-foot-diameter test section of the Lewis altitude wind tunnel. The performance was obtained at rated corrected speed over a range of exhaust-gas temperatures for each of several flight conditions. Variation of exhaust-gas temperature provided data over a range of compressor pressure ratios so that compressor performance could be determined precisely for rated pressure ratio.

Calculations of boundary-layer velocity and suction-surface velocity (just outside the boundary layer) were made with the usual assumption of no static-pressure gradient normal to the wall in the boundary layer. The free-stream value of density was also assumed to exist throughout the boundary layer. The maximum free-stream Mach number for boundary-layer measurements was about 0.6, so the assumption of constant density should be reasonably exact.

SUMMARY OF REYNOLDS NUMBER EFFECTS ON ISOLATED AIRFOILS

The effects of Reynolds number on airfoils are best known through investigations with isolated airfoils. A summary of Reynolds number effects on isolated airfoils is therefore included to aid in the interpretation of compressor boundary-layer phenomena. The pressure gradients and boundary-layer changes are greatest on the suction surface of an airfoil. The review, therefore, will be restricted to the suction surface although it should be kept in mind that the same phenomena exist to a lesser degree on the pressure surface.

Laminar Separation

An idealized variation of boundary-layer thickness (defined as the distance from the airfoil surface to the point where the local velocity is 99 percent of the free-stream velocity) with Reynolds number is shown in figure 3. The flow is completely laminar in the lowest Reynolds number region shown. Because a laminar boundary layer separates rapidly in the presence of an adverse pressure gradient, a large separated region exists from approximately the maximum velocity point to downstream of the trailing edge. Although the thickness of the laminar boundary layer upstream of the separation point varies appreciably with Reynolds number, the thickness of the separation region does not. Hence, at the trailing edge the total boundary-layer thickness varies only slightly with Reynolds number.

Laminar Separation and Turbulent Reattachment

In the next to the lowest Reynolds number range (fig. 3) laminar separation also occurs, but transition to turbulent flow takes place in the separated boundary layer. The transition to turbulent flow is followed by reattachment to the suction surface. The thickness of the reattached turbulent boundary layer is related directly to the height of the separation region so that the presence of a large laminar separation region is undesirable. Reductions in drag can be accomplished by using boundary-layer trippers to cause transition to turbulent flow before laminar separation can take place. This range of Reynolds number is typical of compressor blades operating at altitude conditions; however, it will be shown subsequently that factors other than Reynolds number must be considered for flow in compressors.

Transition Before Separation

The next highest Reynolds number range is characterized by transition from laminar to turbulent flow taking place before significant laminar separation can occur. Because laminar separation is not involved and laminar skin-friction coefficients are smaller than turbulent ones, laminar flow is desirable in this range. The usual methods of preserving laminar flow are to provide a smooth surface on the airfoil and to shape the airfoil so that a favorable pressure gradient exists over much of its surface. This Reynolds number range is typical of many airplane wings.

Turbulent Flow Governed by Surface Roughness

If Reynolds number is increased indefinitely, surface roughness becomes important. In the highest range shown in figure 3, the flow is predominantly turbulent and governed by surface roughness. When the surface roughness extends through the laminar sublayer of the turbulent boundary layer, the boundary-layer thickness becomes independent of Reynolds number. In this range the drag can be reduced only by reducing the surface roughness. Airplane wings that are constructed with many protruding rivet heads are representative of this range. Because compressor blades have small physical dimensions, the relative roughness of dirt deposits and poor surface finish can be quite large. Similar effects of roughness on compressor blades might therefore be expected at lower Reynolds numbers than with airplane wings.

RESULTS AND DISCUSSION

The Reynolds number effects on the over-all compressor are shown in figure 4. As the first-rotor tip Reynolds number was lowered from about

4×10^5 to 3×10^4 , the efficiency decreased from 0.80 to 0.69 and the corrected airflow decreased 10 percent.

Inlet Guide Vanes

It became apparent early in the investigation that laminar separation was taking place on the inlet guide vanes, hence the investigation was extended to include boundary-layer trippers. To facilitate comparison of performance with and without trippers, the results with both inlet-guide-vane configurations are presented simultaneously.

Boundary-layer profiles. - The boundary-layer instrumentation was identical for both the suction and pressure surfaces. Because practically all the pressure-surface boundary layer was between the innermost pressure probe and the blade surface, the data presentation is restricted to the suction surface.

The boundary-layer velocity profiles for the suction surface are shown in figure 5. The boundary-layer velocity and the distance from the blade surface were nondimensionalized; that is, the boundary-layer velocity was divided by free-stream velocity, and the distance from the surface was divided by the chord length. For comparison of the inlet-guide-vane performance to the over-all compressor performance of figure 4, the inlet-guide-vane Reynolds number should be multiplied by three to obtain the approximate first-rotor Reynolds number.

Without tripper wires (fig. 5(a)) the suction-surface boundary layer exhibits extreme changes for the range of Reynolds numbers shown. The shape of the profile at the lowest Reynolds number, with reversed flow probably occurring near the blade surface, indicates separated flow.

With tripper wires (fig. 5(b)) the flow appears attached at all Reynolds numbers. It is evident, however, that the improvement at low Reynolds numbers has been offset by boundary-layer thickening at high Reynolds numbers. Perhaps a more efficient tripper design would reduce this compensating effect.

Suction-surface velocity distribution. - The suction-surface velocity distributions for the inlet guide vanes are shown in figures 6 and 7. The suction-surface velocity, of course, is the free-stream velocity just outside the boundary layer on the suction surface.

Without trippers (fig. 6) a large difference exists between the high and low Reynolds number distribution. At the high Reynolds number, a conventional profile is obtained. At the low Reynolds number, however, a large constant-pressure, constant-velocity region is found. This flat spot results from the inability of the separated laminar boundary layer

to withstand diffusion, hence the pressure and velocity just outside the boundary layer remain constant. The large extent of the laminar separation region at a Reynolds number of about 1×10^4 (fig. 6(b)) agrees with the separated boundary-layer profile of figure 5(a) for about the same Reynolds number. Laminar separation regions were also obtained at intermediate Reynolds numbers but, as a result of turbulent reattachment, were much less extensive.

With the tripper wires (fig. 7) the difference between the high and low Reynolds number velocity distributions is much smaller. The use of tripper wires greatly reduces or eliminates the laminar separation region.

The difference between the two high Reynolds number distributions (figs. 6(a) and 7(a)) is attributed to the presence of the tripper wire, which would modify the velocity distribution.

Thus, in examining the flow on the inlet guide vanes, substantial agreement with isolated airfoil experience has been found. Without trippers, laminar separation and turbulent reattachment was found on the inlet guide vanes with completely separated flow at the lowest Reynolds number investigated. The use of trippers greatly reduced or eliminated laminar separation at low Reynolds numbers but increased the boundary-layer thickness slightly at high Reynolds numbers. The presence of laminar separation on inlet guide vanes and its prevention with tripper wires has been substantiated by unpublished data for other compressors.

Effect of inlet-guide-vane trippers on compressor performance. - The effect of inlet-guide-vane trippers on compressor performance is shown in figure 8. The first-stage efficiency, over-all efficiency, and corrected airflow are plotted against first-rotor Reynolds number for operation both with and without tripper wires. From the performance standpoint it was convenient to group the first rotor with the inlet guide vanes to obtain first-stage performance. Whether or not laminar separation occurs on the first-rotor blades is not known as there was no instrumentation on these blades. Since the first-stage pressure and temperature rise are small, the efficiency (fig. 8(a)) has considerable scatter. However, it is evident that the trippers improved the efficiency of the first stage at low Reynolds numbers.

Because the first stage contributes only a small portion of the total work, the effect of trippers on the over-all compressor efficiency is much smaller (fig. 8(b)). At low Reynolds numbers the over-all efficiency is about 1 or 2 percent higher with the trippers, but at high Reynolds numbers a decrease of about 1 percent was observed. The decrease at high Reynolds numbers is probably the result of the thicker inlet-guide-vane boundary layer with trippers as was shown in figure 5(b). The airflow (fig. 8(c)) was increased about 1 or 2 percent at low Reynolds numbers by the use of trippers and was unchanged at high Reynolds numbers.

Effect of Turbulence

Before examining the first-stator data the difference in turbulence level should be considered. Within the compressor a high level of turbulence exists. It is well known that the velocities in the blade wakes at the entrance to the next blade row are 20 to 30 percent lower than free-stream velocities. The wakes therefore represent a high turbulence level for the next blade row. The data of figure 9, which show an order of magnitude for the effect of turbulence, were obtained from reference 1 and are for transition on a flat plate.

For simplicity, the transition from laminar to turbulent flow is often considered to take place at a single point. As shown in figure 9, however, the actual transition occurs over a finite length. At low turbulence levels (below about 0.1 percent) the location of transition is independent of turbulence level. In this range the natural instability of the laminar boundary layer is sufficient to cause transition to turbulent flow. At higher turbulence levels, however, an increase in turbulence is accompanied by a decrease in transition Reynolds number. The data stop far short of the possible 20- or 30-percent turbulence level of a compressor. The wakes represent highly nonisotropic turbulence, so direct numerical comparisons to the effects of isotropic turbulence shown in figure 9 cannot be made. However, the trend indicates that a first-order effect of turbulence can be expected within the compressor.

The turbulence level of the flow ahead of the inlet guide vanes was not measured, but a settling chamber with screens followed by flow contraction was used ahead of the engine. Hence, a turbulence level of the order of 1 percent might be expected.

First Stator

Boundary-layer profiles. - Unlike the inlet-guide-vane profiles, the pressure-surface boundary layer of the first stator extended well beyond the innermost probe, so profiles are presented for both suction and pressure surfaces in figure 10. The equivalent first-rotor Reynolds numbers can be obtained by multiplying the first-stator Reynolds numbers by two.

The coordinates of figure 10 are the same as those used for figure 5, velocity divided by free-stream velocity and distance from blade surface divided by chord length. The thicknesses of both the suction- and pressure-surface boundary layers increased with decreasing Reynolds number, but the greatest change was obtained on the suction surface. Although the boundary layer becomes quite thick on the suction surface at low Reynolds numbers, it does not appear separated.

The suction-surface boundary layers at the two lowest Reynolds numbers extend over enough instrumentation so that the complete boundary-layer profiles were approximated. From these boundary-layer profiles

the displacement thickness $\hat{\delta}^*$, the momentum thickness $\hat{\theta}$, and the form factor H ($H = \hat{\delta}^*/\hat{\theta}$) were calculated.

The value of the form factor H was about 2.0 for the two lowest Reynolds number profiles of figure 10(b). These profiles were plotted in figure 11 together with a typical turbulent profile for $H = 2.0$ from reference 2. In figure 11 the abscissa was nondimensionalized by dividing by the momentum thickness $\hat{\theta}$. As can be seen, the agreement between the data and the turbulent profile is excellent, indicating essentially turbulent flow on the first stator.

Thus, the flow on the suction surface is apparently turbulent, but the pressure surface must be considered also. The pressure-surface boundary layers were too thin to make accurate estimates of the shape (fig. 10(a)). The data of reference 1, however, indicate that laminar flow on a concave surface (the pressure surface) is more unstable than flow on a convex surface (the suction surface). Hence, if turbulent flow occurs on the suction surface, the flow on the pressure surface should also be turbulent.

Suction-surface velocity distribution. - The suction-surface velocity distributions for the first stator are shown in figure 12. The difference between the high and low Reynolds number velocity distributions (figs. 12(a) and (b)) results indirectly from the variation of corrected airflow with Reynolds number. The change in corrected airflow causes a small change in angle of attack which, in turn, causes the difference in velocity distribution. There is, however, no indication of laminar separation, which is further evidence of predominantly turbulent flow. Obviously, boundary-layer trippers would be of no value on the first-stator blades.

First-stator profile losses. - One measurement of cascade losses is the buildup of boundary-layer momentum thickness through a cascade. The wake momentum thicknesses of two-dimensional compressor cascades were correlated with a suction-surface diffusion ratio in reference 3 for a wide range of configurations. The mean line from the correlation at mid-range (approximately minimum loss) angle of attack is reproduced from reference 3 in figure 13. The correlation of reference 3 varies slightly with angle of attack, but the single correlation line in figure 13 is accurate enough for the purposes of this discussion.

Also shown in figure 13 are the first-stator momentum thicknesses (calculated from the boundary-layer profiles of fig. 10) for various

Reynolds numbers.¹ The first-stator momentum thicknesses vary from about 2.7 to 5.8 times the two-dimensional correlation values for the same diffusion ratios. However, the first-stator data were obtained over a wide range of Reynolds numbers, thus a large amount of the spread from 2.7 to 5.8 can be attributed to Reynolds number effects. In order to reduce this spread, the effect of Reynolds number on the boundary-layer thickness must be considered.

The relationship between boundary-layer thickness and Reynolds number is often expressed as

$$\delta^* = K(\rho V_0 x / \mu)^n$$

where the value of n for turbulent flow at low Reynolds numbers is usually $-1/5$ (ref. 4).

The one-fifth power relation was used as an approximate correction for Reynolds number effects. The first-stator data, corrected to the Reynolds number of the two-dimensional correlation (2.3×10^5), are shown by the solid symbols in figure 13. After correction, the first-stator momentum thicknesses are still 2.6 to 3.4 times the correlation values. Some of the remaining difference might be explained in terms of Mach number and extent of laminar flow, as the cascade correlation data were obtained at low Mach numbers in low-turbulence duct tests. However, a factor of about two is still left unexplained.

Although the first-stator instrumentation was not complete enough to draw accurate quantitative conclusions, it is evident that the first-stator midspan losses were substantially greater than the two-dimensional cascade losses. A possible cause of the high losses on the first stator was the presence of blade wakes from the preceding blade row. A 20- to 30-percent deficit in wake velocity corresponds to a 10° to 20° change in angle of attack at the entrance of a blade row. Thus, the impingement of first-rotor wakes on the first-stator blade row could cause localized, intermittent stalling, with the boundary-layer instrumentation indicating some mean flow condition. Of course, separating the blade rows by a longer mixing length would decrease the wakes, but the turbulence level would also decrease so that laminar separation might occur.

Thus, the midspan flow on the first stator differs markedly from both the isolated airfoil experience and the inlet-guide-vane data. The flow was predominantly turbulent even at the lowest Reynolds numbers investigated. Boundary-layer trippers were not installed on the first stator because there was no evidence of laminar separation. The magnitude

¹The boundary-layer instrumentation and the downstream suction-surface static orifice were located at about the 81-percent-chord position. Therefore, a chord length of about 1.13 inches was used to calculate Reynolds number and the momentum thickness ratio for figure 13 instead of the actual chord length of about 1.4 inches.

of the midspan losses was much greater than two-dimensional cascade losses, perhaps because of the wakes from the preceding rotor blades.

Over-All Compressor

From the standpoint of Reynolds number and turbulence level, predominantly turbulent flow might be expected on all rotors and stators after the first stator row. As mentioned in the preceding section, the thickness of a turbulent boundary layer varies inversely as about the one-fifth power of Reynolds number. With turbulent flow over the first stator and all following blade rows, the loss in this portion of the compressor might therefore be expected to vary inversely as the one-fifth power of Reynolds number. For a measure of loss, $1 - \eta$ was used. This loss parameter is plotted against a first-stator Reynolds number in figure 14(a) for stages 2 to 13. Since, for a given corrected speed and pressure ratio, all chord Reynolds numbers through the compressor are approximately proportional to each other, the particular choice of Reynolds number for the abscissa is immaterial.

As can be seen in figure 14(a), the data agree with the slope from the turbulent-boundary-layer equation except at the highest Reynolds numbers, thus tending to substantiate the assumption of predominantly turbulent flow on these blade rows. The departure from the slope of $-1/5$ at high Reynolds numbers is attributed to roughness from either the blade manufacturing process or dirt deposits. If data were available at much higher Reynolds numbers for this compressor, a mean line for the data would be expected to approach a slope of zero. This tentative explanation of compressor Reynolds number effects in terms of turbulent-boundary-layer theory ignores tip and hub flow phenomena. Obviously, a rigorous explanation of Reynolds number effects would require knowledge of flow in the hub and tip regions.

In the discussion of the inlet guide vanes, it was pointed out that the first stage contributed only a small portion of the work done by the complete compressor. Hence, the loss for the complete compressor should follow a trend similar to figure 14(a). The loss for the complete compressor is plotted in figure 14(b). The data again follow the turbulent slope except at high Reynolds numbers. Unpublished data from other compressor investigations show similar trends to those in figure 13. The agreement with turbulent-boundary-layer theory indicates that trippers would be of little value except on the first one or two blade rows.

CONCLUDING REMARKS

The flow on the inlet guide vanes was similar to isolated airfoil experience in that laminar separation and turbulent reattachment took

place at low Reynolds numbers. Completely separated flow was observed at the lowest Reynolds number investigated.

The use of trippers reduced or prevented laminar separation on the inlet guide vanes, but the improvement in over-all compressor performance was small because only one or two blade rows was involved. Also, at least with the tripper configuration used, a small performance penalty was involved at high Reynolds numbers.

The turbulence level within the compressor caused the midspan flow of the first stator to be predominantly turbulent even at the lowest Reynolds numbers investigated. The use of trippers for all blade rows therefore does not appear promising.

The first-stator profile losses at the midspan position were substantially greater than the two-dimensional cascade losses. The high losses possibly result from the impingement of wakes from the preceding blade row.

The over-all compressor losses vary inversely as about the one-fifth power of Reynolds number, except at high Reynolds numbers where surface roughness apparently tends to reduce the effects of Reynolds number. As a tentative conclusion then, it appears that turbulent-boundary-layer theory explains the variation of compressor efficiency with Reynolds number. Before this conclusion can be put on a firm basis, a better understanding of loss mechanisms is needed, particularly the nature and importance of hub and tip losses.

Lewis Flight Propulsion Laboratory
National Advisory Committee for Aeronautics
Cleveland, Ohio, April 10, 1957

REFERENCES

1. Gazley, Carl, Jr.: Boundary-Layer Stability and Transition in Subsonic and Supersonic Flow. Rep. No. R52A0506, Apparatus Dept., General Electric Co., May 1952. (Proj. Hermes TUL-2000A, Contract DA-30-115-ORD-23.)
2. Sandborn, Virgil A.: Preliminary Experimental Investigation of Low-Speed Turbulent Boundary Layers in Adverse Pressure Gradients. NACA TN 3031, 1953.
3. Lieblein, Seymour: Analysis of Experimental Low-Speed Loss and Stall Characteristics of Two-Dimensional Compressor Blade Cascades. NACA RM E57A28, 1957.
4. Dodge, Russell A., and Thompson, Milton J.: Fluid Mechanics. McGraw-Hill Book Co., Inc., 1937.

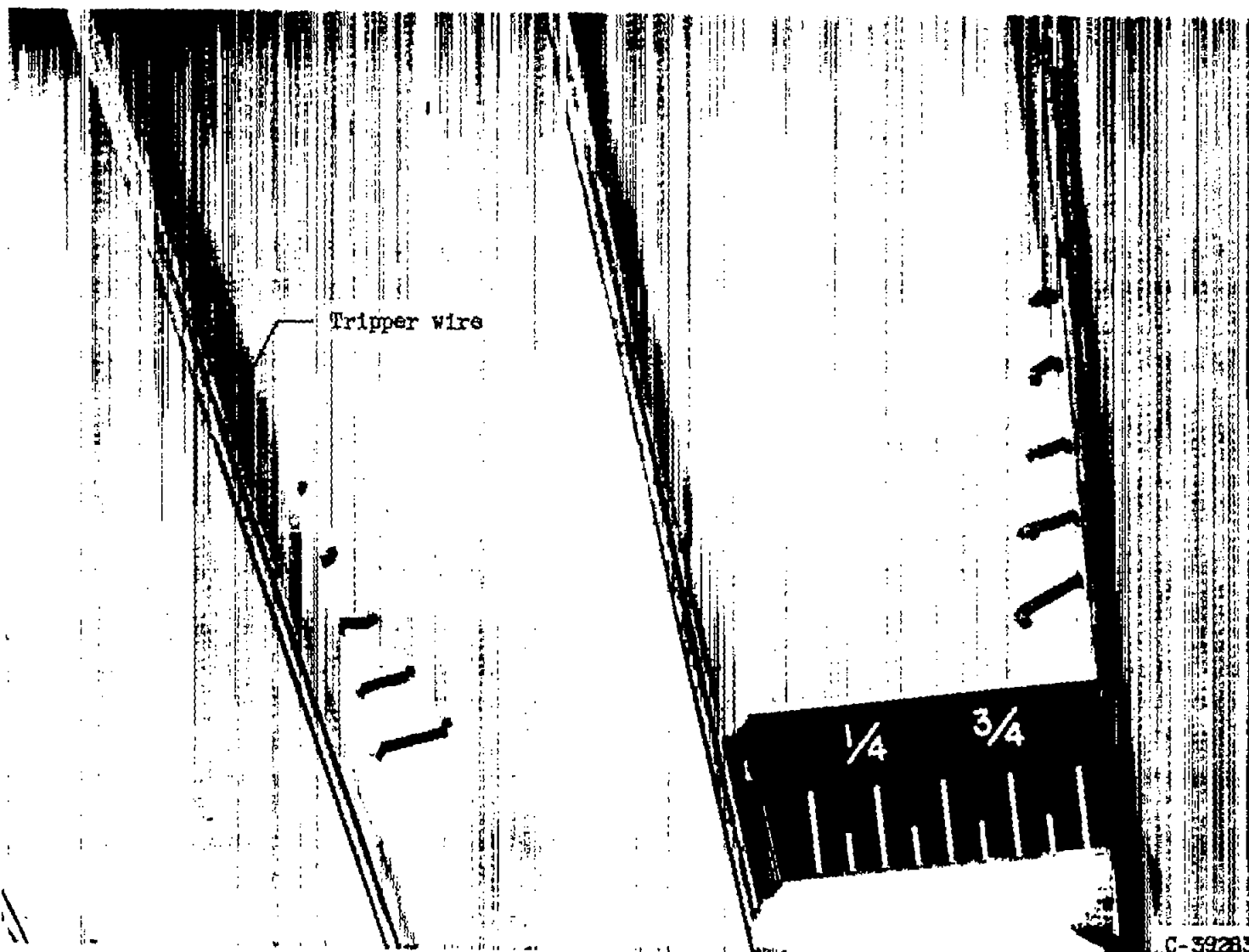


Figure 1. - Boundary-layer instrumentation on inlet guide vanes.

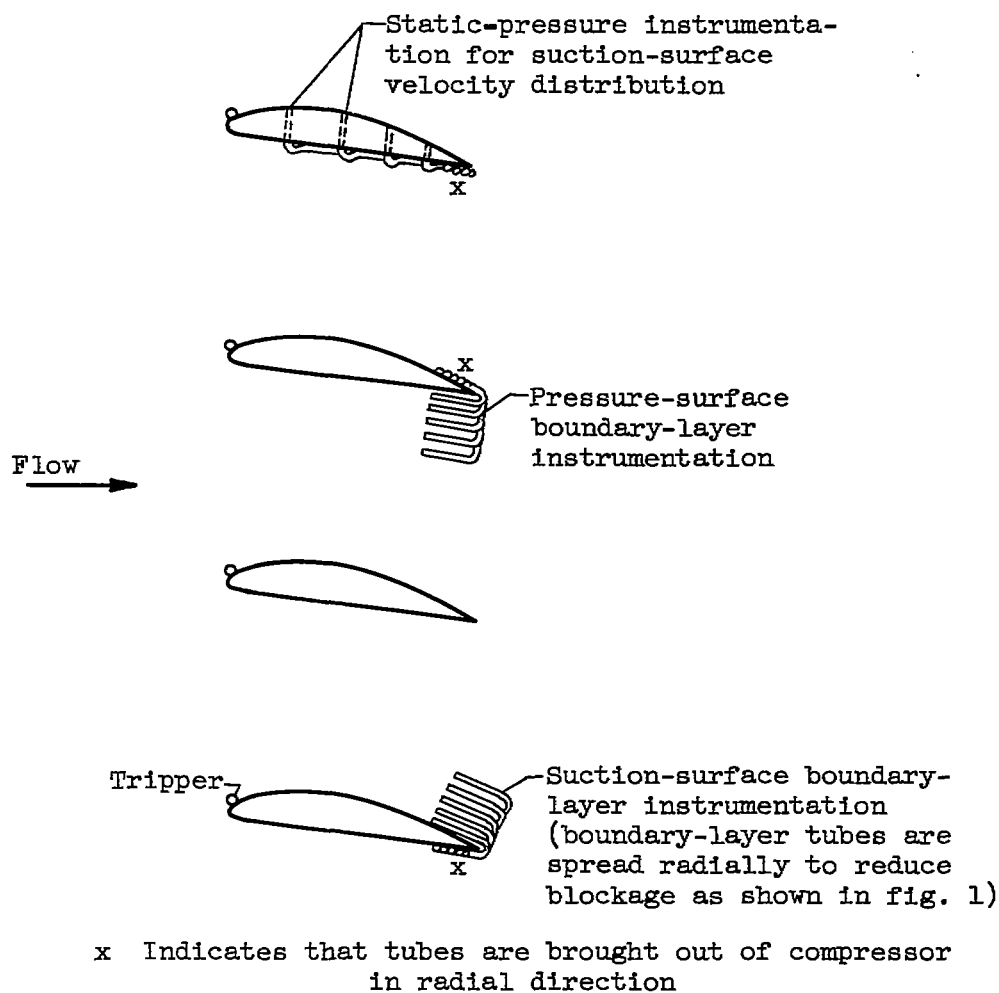


Figure 2. - Sketch of inlet-guide-vane instrumentation (not to scale).

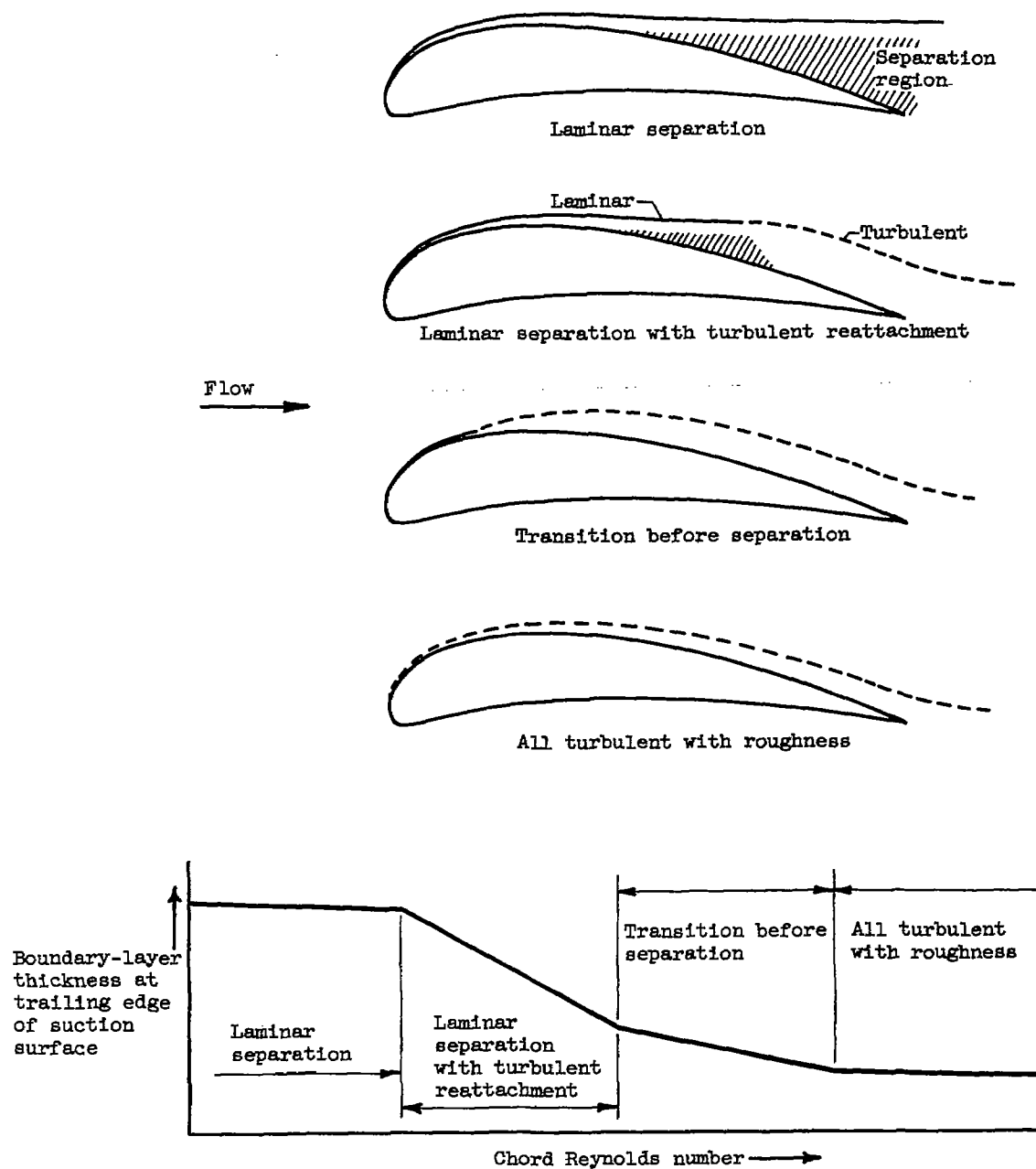


Figure 3. - Idealized variation of boundary-layer thickness with Reynolds number for an isolated airfoil.

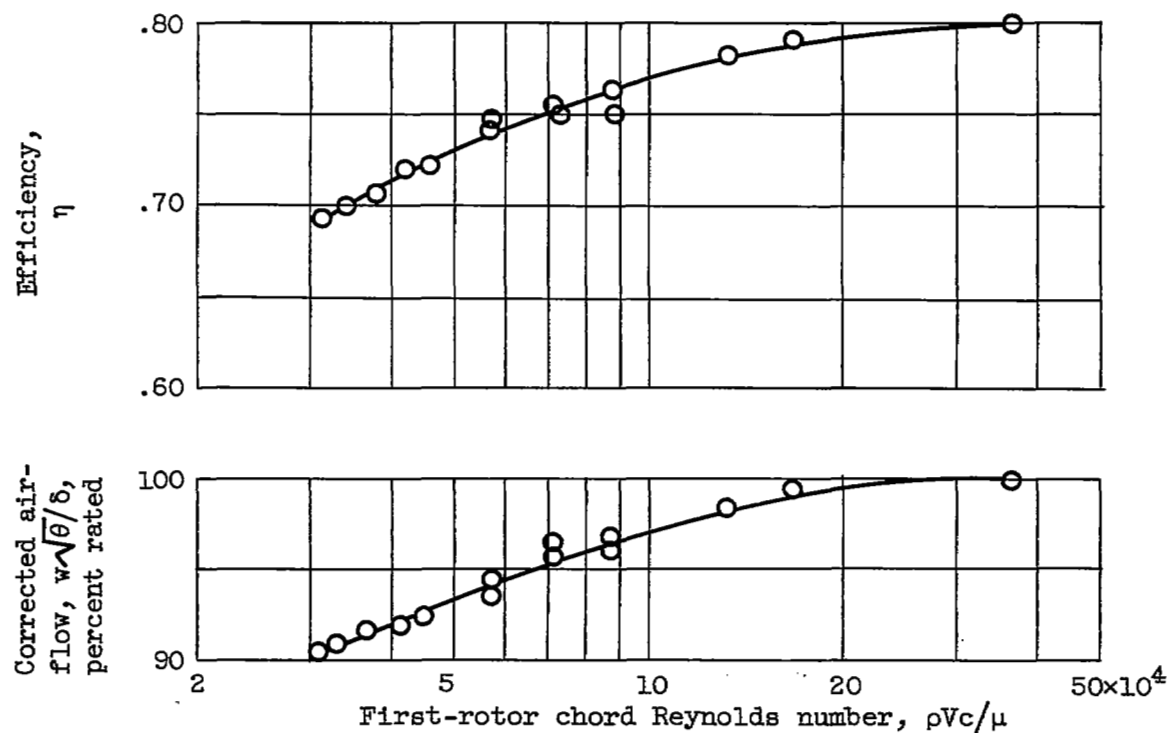
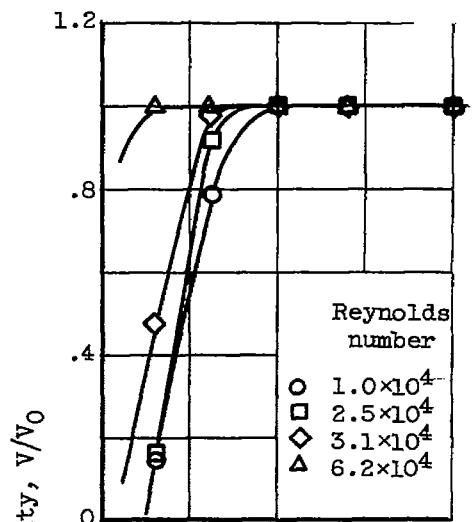
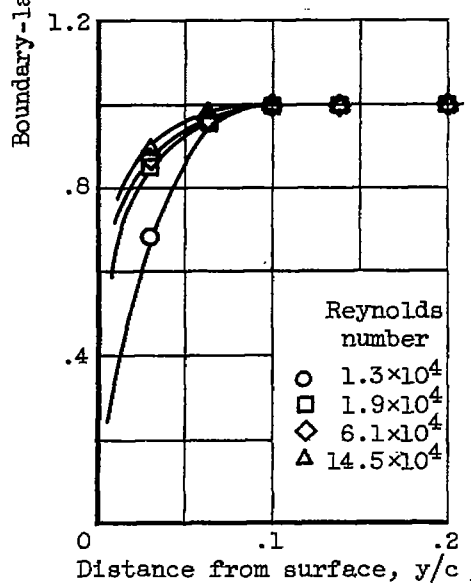


Figure 4. - Effect of Reynolds number on compressor performance at rated corrected speed and rated pressure ratio.



(a) Without tripper wires.



(b) With tripper wires.

Figure 5. - Boundary-layer profiles for inlet guide vanes (suction surface only).

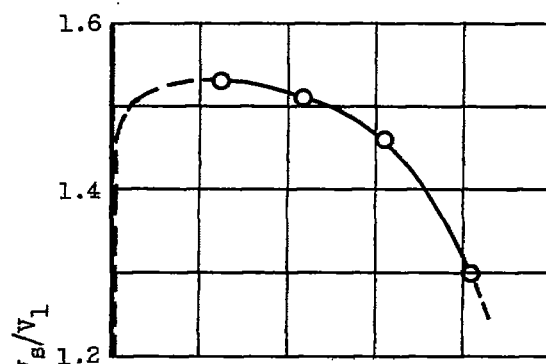
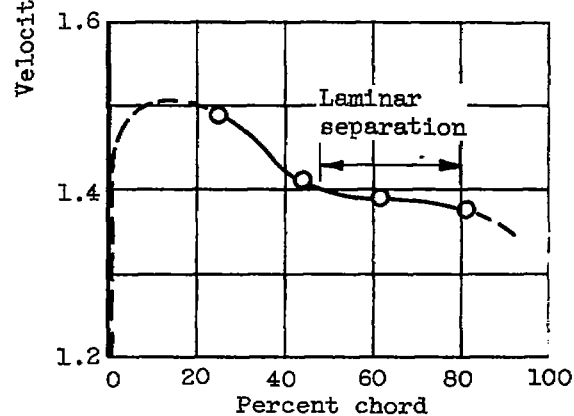
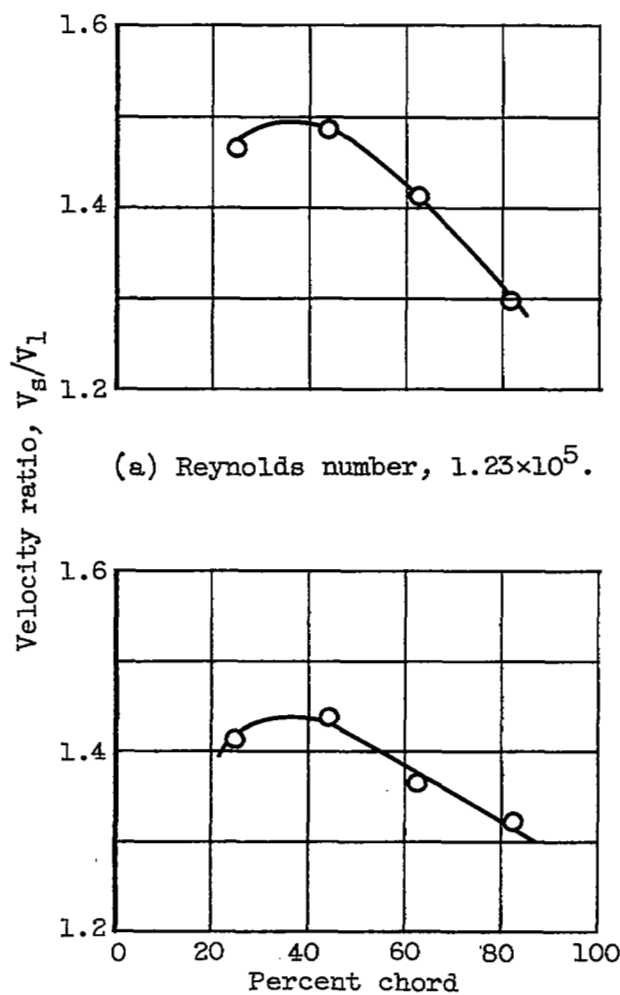
(a) Reynolds number, 1.8×10^5 .(b) Reynolds number, 1.1×10^4 .

Figure 6. - Inlet-guide-vane suction-surface velocity profiles without tripper wires.



(b) Reynolds number, 1.3×10^4 .

Figure 7. - Inlet-guide-vane
suction-surface velocity
profiles with tripper wires.

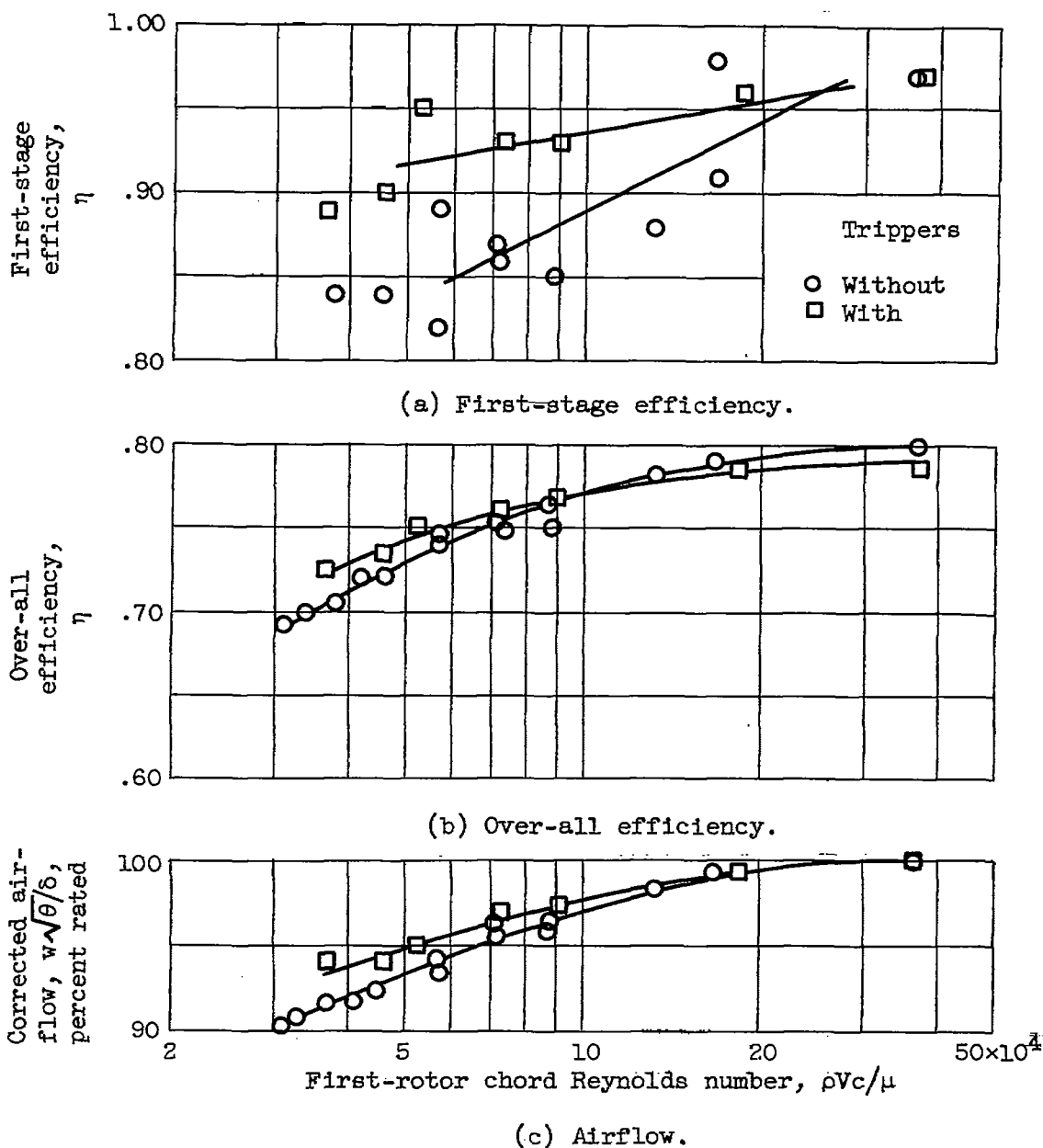


Figure 8. - Comparison of compressor performance with and without boundary-layer trippers on inlet guide vanes.

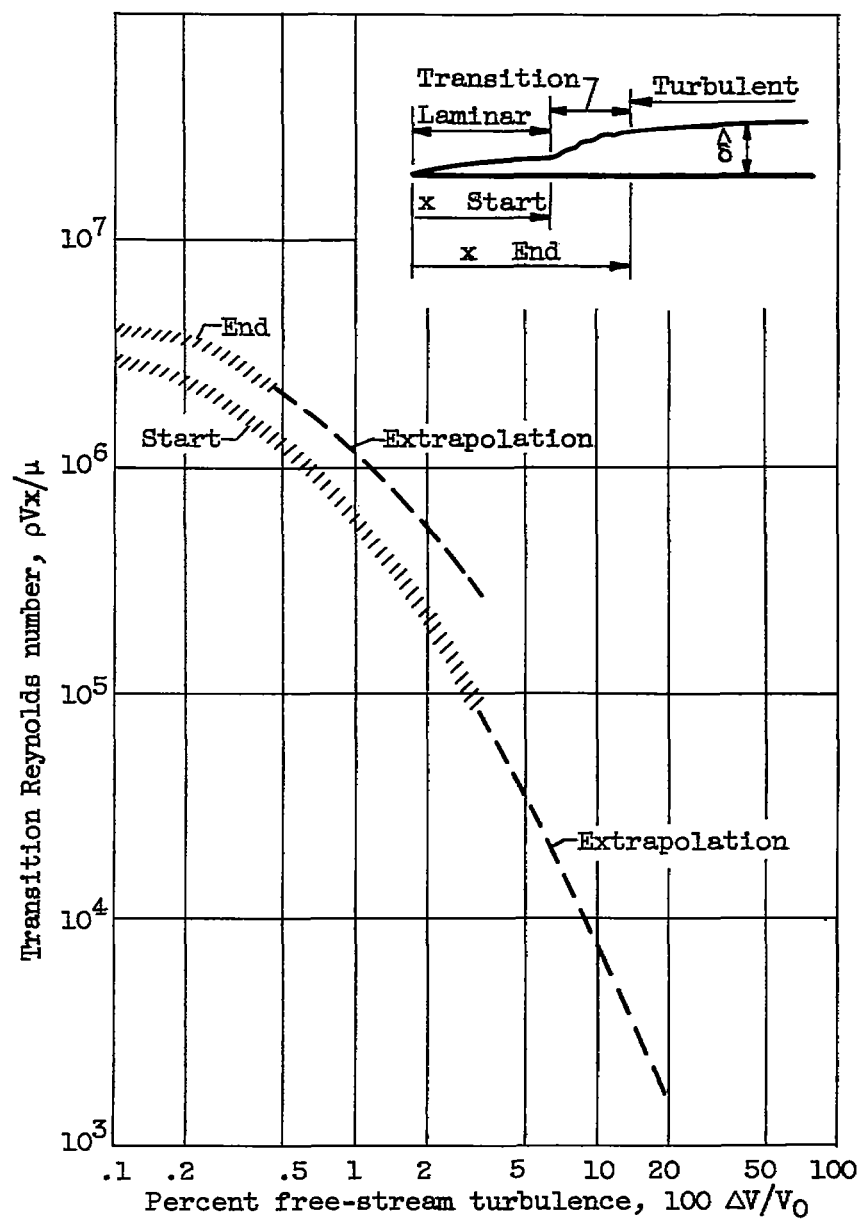
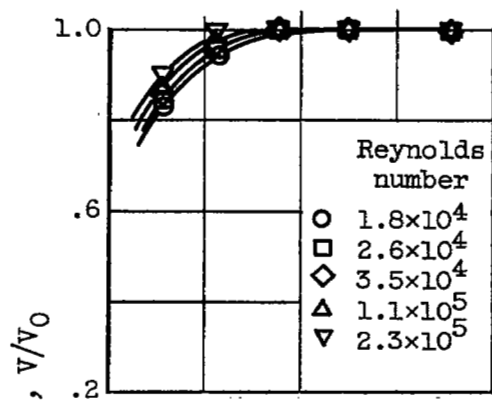
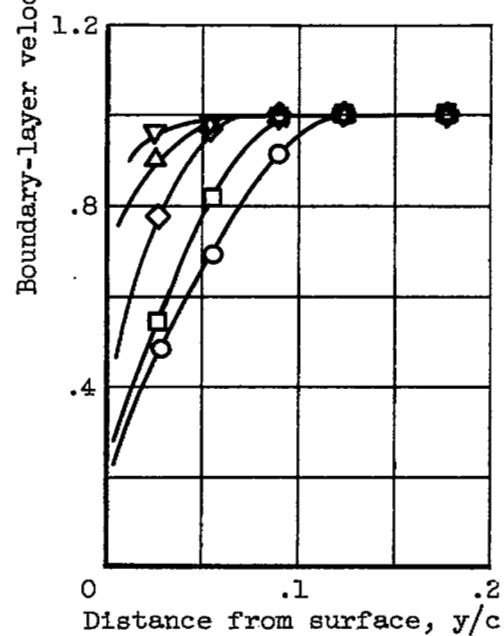


Figure 9. - Effect of turbulence level on flat-plate transition Reynolds number.



(a) Pressure surface.



(b) Suction surface.

Figure 10. - Boundary-layer profiles for first stator.

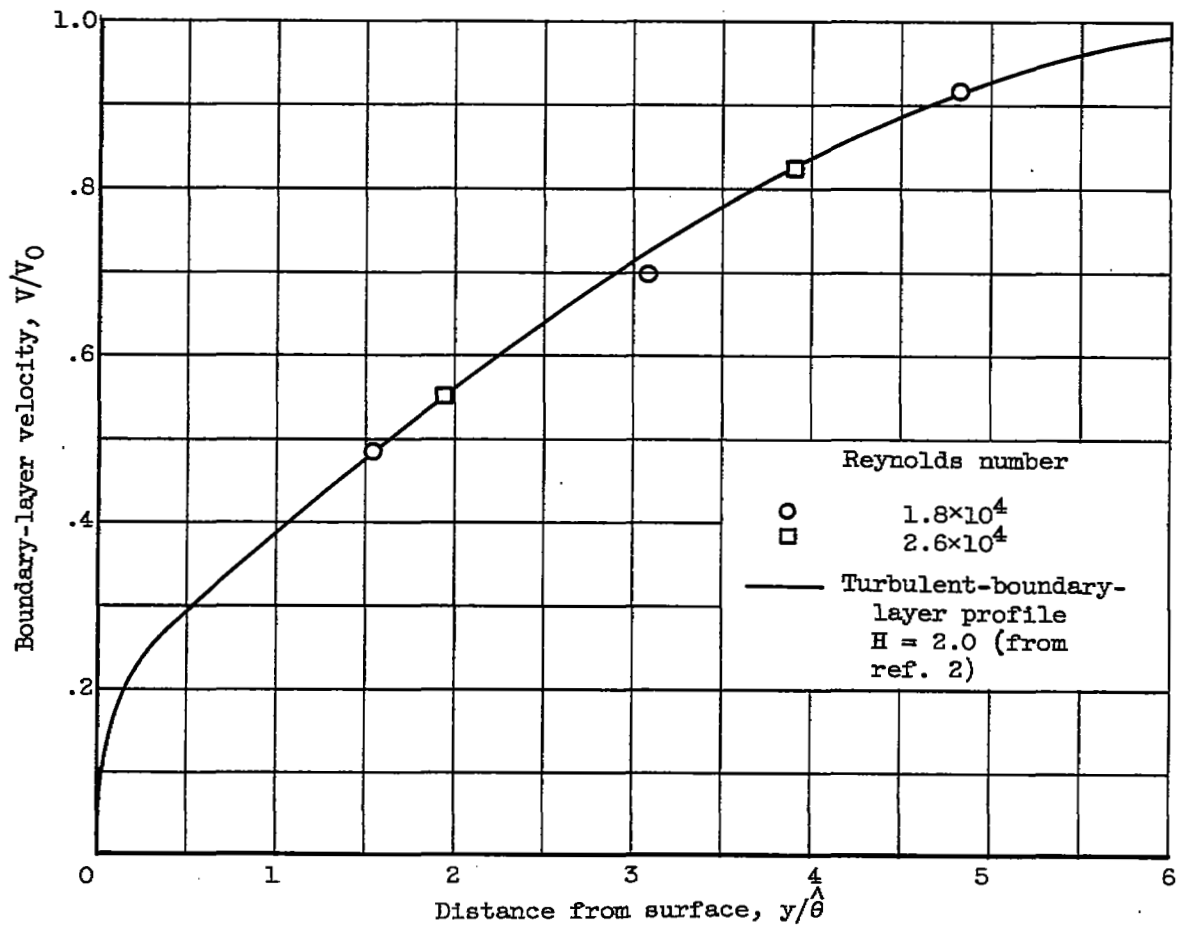
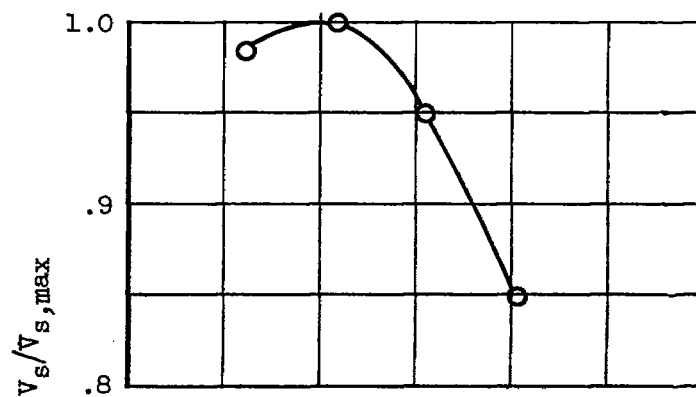
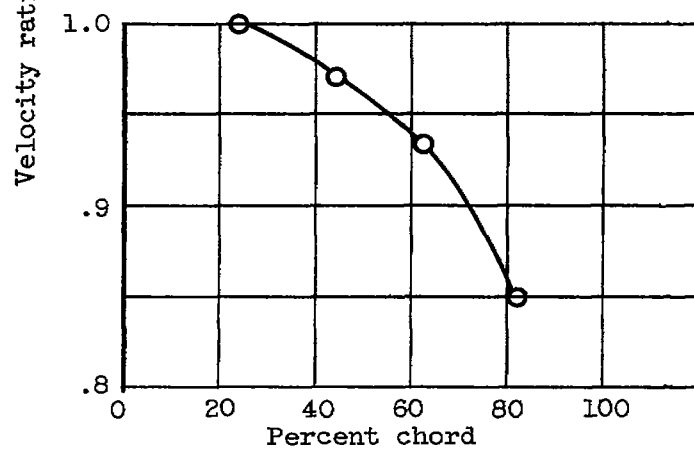


Figure 11. - Comparison of first-stator suction-surface velocity profiles with a turbulent-boundary-layer profile from reference 2.



(a) Reynolds number, 3.2×10^5 .



(b) Reynolds number, 2.0×10^4 .

Figure 12. - First-stator
suction-surface velocity
profiles.

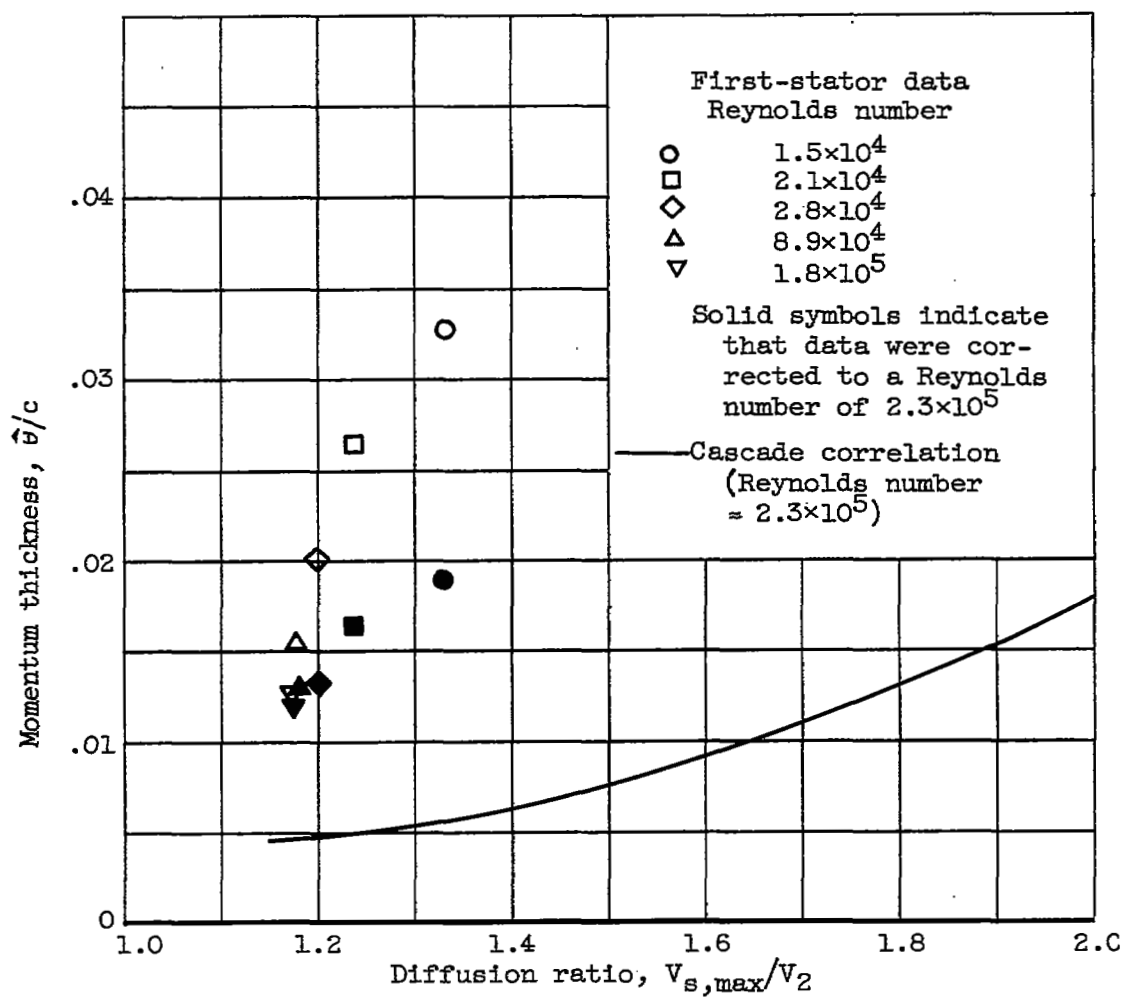
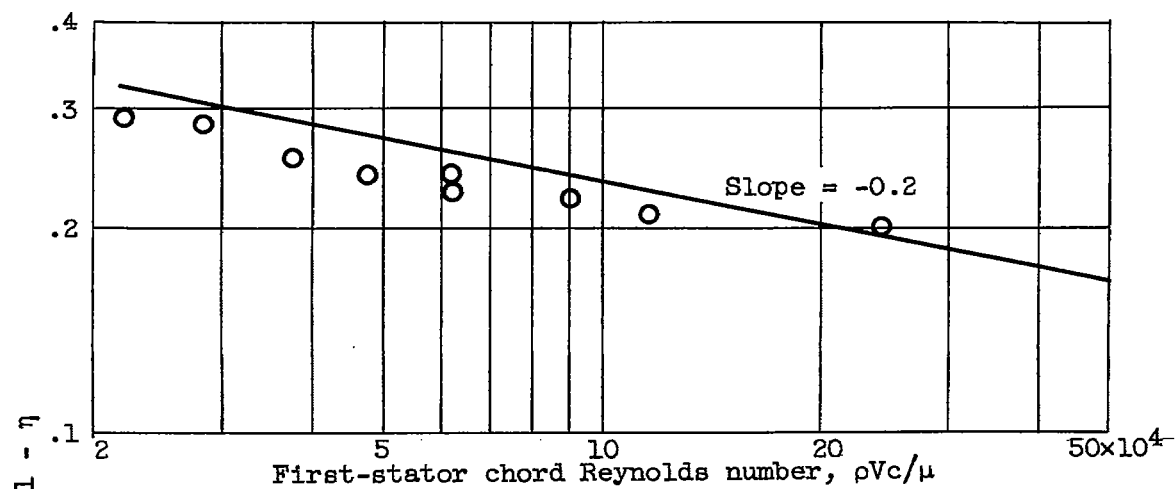
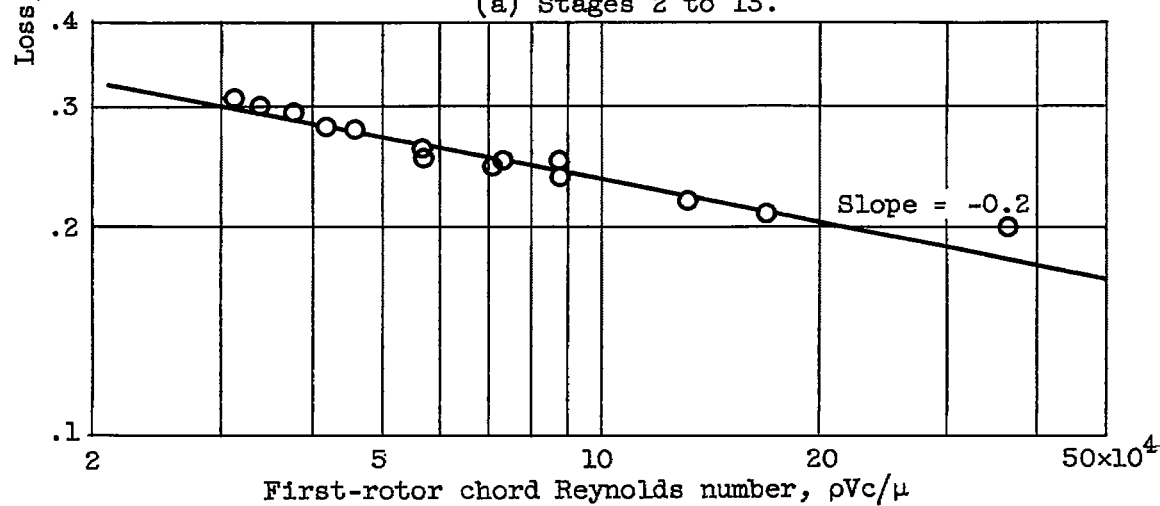


Figure 13. - Comparison of midspan first-stator losses with two-dimensional-cascade correlation of reference 3.



(a) Stages 2 to 13.



(b) Over-all compressor.

Figure 14. - Variation of loss with Reynolds number for compressor.



3 1176 01351 8080

1111 1111 1111

1111 1111 1111